scientific reports

Check for updates

OPEN

Screening and identification of miRNAs negatively regulating FAM83A/Wnt/β-catenin signaling pathway in non-small cell lung cancer

Wenbin Yuan[1], Wei Liu[1], Huili Huang[1], Xingyu Chen[1], Rui Zhang[1], Hao Lyu[1], Shuai Xiao[1], Dong Guo[1], Qi Zhang[1], Declan William Ali[3], Marek Michalak[4], Xing-Zhen Chen[2], Cefan Zhou[1]✉ & Jingfeng Tang[1]✉

The prevalence of non-small cell lung cancer (NSCLC) accounts for 85% of all lung cancers, with the Wnt/β-catenin signaling pathway exhibiting robust activation in this particular subtype. The expression of FAM83A (family with sequence similarity 83, member A) has been found to be significantly upregulated in lung cancer, leading to the stabilization of β-catenin and activation of the Wnt signaling pathway. In this study, we conducted a screening of down-regulated miRNAs in lung cancer with FAM83A as the target. Ultimately, we identified miR-1 as a negative regulator of FAM83A and confirmed that FAM83A is a direct target gene of miR-1 through dual luciferase reporter assays. The overexpression of miR-1 significantly attenuated the expression level of FAM83A and suppressed the Wnt signaling pathway, leading to a reduction in the expression levels of downstream target genes AXIN2, CyclinD1, and C-MYC. Additionally, it decreased the nuclear translocation of β-catenin. In addition, overexpression of miR-1 accelerated the degradation of β-catenin by inhibiting FAM83A, promoted the assembly of β-catenin degradation complex, and inhibited the proliferation, migration and invasion of NSCLC cells. In summary, miR-1 may be a potential candidate miRNA for the treatment of NSCLC.

Keywords Non-small cell lung cancer, FAM83A, miR-1, Wnt/β-catenin

The Wnt/β-catenin signaling pathway is known to undergo activating mutations in various cancers. However, β-catenin and APC mutations are uncommon in non-small cell lung cancer (NSCLC). Despite this, the Wnt/β-catenin signaling pathway still plays a crucial role in maintaining the proliferation of NSCLC cell lines, and inhibition of this pathway can significantly slow down the NSCLC process[1]. As a result of the suppression of the degradation complex in the activated Wnt signaling pathway, β-catenin that has been stabilized is transported into the nucleus and triggers the transcription of target genes downstream through its interaction with T cell factor (TCF)/lymphoid enhancer binding factor (LEF), which are transcription factors[2]. FAM83A, also known as BJ-TSA-9, exhibits significant upregulation in cases of lung carcinoma[3]. In our previous work, we found that FAM83A, through its the DUF1669 domain directly interacts with Arm repeats domain of β-catenin and promotes β-catenin nuclear transports to initiate transcription of target genes downstream of Wnt. Repression of FAM83A led to notable suppression of cellular growth, indicating that targeting FAM83A could be a promising strategy for cancer treatment[4].

[1]Key Laboratory of Fermentation Engineering (Ministry of Education), National "111" Center for Cellular Regulation and Molecular Pharmaceutics, Cooperative Innovation Center of Industrial Fermentation (Ministry of Education and Hubei Province), Hubei Key Laboratory of Industrial Microbiology, School of Life and Health Sciences, Hubei University of Technology, Wuhan 430068, People's Republic of China. [2]Membrane Protein Disease Research Group, Department of Physiology, Faculty of Medicine and Dentistry, University of Alberta, Edmonton, AB, Canada. [3]Department of Biological Sciences, University of Alberta, Edmonton, AB, Canada. [4]Department of Biochemistry, University of Alberta, Edmonton, AB, Canada. ✉email: cefan@hbut.edu.cn; Jingfeng_hut@163.com

RNA-based therapies show promise in treating diseases that are currently considered incurable with conventional therapies[5]. RNA-based therapeutics have been utilized in clinical treatments with the development of RNA delivery technology[6]. Among them, microRNAs (miRNAs) represent a pivotal class of gene regulators. These small RNA sequences have a pivotal function in regulating the expression of target genes[7,8]. The dysregulation of miRNAs is a key characteristic that distinguishes cancer cells from normal cells. This is particularly evident in the decreased expression of miRNAs that have oncogenic effects and the increased expression of miRNAs that have anti-oncogene effects. Additionally, miRNA expression profiles vary across different types of cancer[9]. miRNAs most typically regulate mRNA stability directly at the RNA level by recognizing sites in the 3′ untranslated region (UTR)[10]. miRNAs have a significant impact on gene expression, and any perturbation of miRNA expression may affect the stability of target genes and thus cellular homeostasis. Therefore, miRNA screening and application have become crucial areas of basic and translational biomedical research[11]. This study focuses on the potential of miRNA gene therapy for lung cancer treatment. In particular, the miRNA screening focused on FAM83A, and it was observed that miR-1 effectively suppressed the Wnt/β-catenin signaling pathway by targeting FAM83A. Consequently, this inhibition resulted in a notable reduction in the proliferation of lung cancer cells. The miR-1 exhibits high conservation across mammalian cells and demonstrates low expression levels within various tumor cell types, suggesting its potential role as a tumor suppressor[12]. Therefore, miR-1 is a promising and effective miRNA for lung cancer therapy.

Result

Identification of miR-1 as a negative regulator of FAM83A in human lung cancer

To identify miRNAs that were downregulated in lung cancer, we analyzed miRNA arrays of lung adenocarcinoma, squamous cell lung cancer, and pan lung cancer in the TCGA database (Data download from https://portal.gdc.cancer.gov/), and finally screened 16 miRNAs that were significantly downregulated in all types of lung cancer (Figs. 1A,B, S1A,B). In addition, the TCGA lung cancer database revealed a significantly elevated expression of FAM83A in tumor tissues compared to adjacent tissues (Analyzed by using GEPIA website: http://gepia.cancer-pku.cn/) (Fig. 1C). Considering the significance of FAM83A in lung cancer, we predicted the potential miRNAs targeting FAM83A in the miR-Walk (http://mirwalk.umm.uni-heidelberg.de/), miRanda (http://www.microrna.org/), and Targetscan (https://www.targetscan.org/) databases, respectively, and screened 331 miRNAs potentially targeting FAM83A mRNA. After merging the aforementioned collections, five miRNAs were finally screened through the database that were down-regulated in lung cancer and targeted FAM83A. These miRNAs are miRNA-143, miRNA-486, miRNA-140, miRNA-1, and miRNA-490 (Fig. 1D). Survival analysis was performed for FAM83A and the five miRNAs (Figs. 1E,F, S2A–D). The results indicated that the downregulation of all miRNAs, except miRNA-143, significantly worsened the prognosis of lung cancer patients.

FAM83A is a target of miR-1

We synthesized and transfected above potential miRNAs targeting FAM83A in 293 T cells. The findings indicated that the upregulation of miR-1 resulted in a notable decrease in the levels of FAM83A, indicating its promising role as a proficient miRNA for modulating the expression of FAM83A (Fig. 2A,B). We made a prediction on the seed sequence located in the 3'UTR and introduced mutations to confirm the direct targeting site of FAM83A mRNA by miR-1. Additionally, we employed a dual luciferase reporter gene system to assess the binding capacity of miR-1 towards the specific region (212-219) within FAM83A 3′UTR (Fig. 2C). In the dual-luciferase assay, the relative luciferase activity is used to measure the regulatory effect of miR-1 on the FAM83A 3′UTR. A decrease in relative luciferase activity indicates that miR-1 is binding to the target site on the FAM83A 3′UTR, leading to repression of gene expression. The findings indicated that the seed sequence of the FAM83A 3'UTR can be directly targeted by miR-1, while the mutated FAM83A 3′UTR cannot be targeted by miR-1 (Fig. 2D). Moreover, a noteworthy inverse association was observed between the levels of miR-1 and FAM83A mRNA in the TCGA database, which was further validated through RT-qPCR analysis (Fig. 2E, F). These findings indicate that FAM83A is subject to direct negative regulation by miR-1.

miR-1 decreases Wnt/β-catenin signal through FAM83A

In a previous study, it was found that FAM83A promotes the stability of β-catenin and initiates the activation of the Wnt/β-catenin signaling pathway. So, we hypothesized that miR-1 expression inhibits the Wnt signaling pathway through FAM83A. In A549 and H1299 cell lines, we observed a significant reduction in the protein levels of Wnt downstream target genes C-MYC, CyclinD1, and AXIN2 upon overexpression of miR-1. However, when FAM83A was reintroduced, it effectively reversed the suppression of Wnt target genes caused by miR-1 overexpression (Fig. 3A). Next, we employed the TCF/LEF transcription factor system labeled with EGFP and mCherry to evaluate the activity of Wnt pathway promoters (Fig. 3B). The data showed that the number of green puncta was significantly reduced when miR-1 was overexpressed (Fig. 3C,D). However, the decrease could potentially be counteracted by re-expressing the FAM83A. Comparable results were observed when measuring mRNA levels of C-MYC, CyclinD1, and AXIN2 using RT-qPCR (Fig. 3E–J). These results indicate that miR-1 may have a negative regulation on the Wnt/β-catenin signaling pathway by targeting FAM83A.

In addition, the TCF/LEF promoter is bound by nuclear β-catenin, which triggers the activation of downstream target genes in the Wnt/β-catenin pathway. Consequently, the importation of β-catenin into the nucleus serves as a significant indicator for Wnt/β-catenin pathway activation. In this study, we evaluated the levels of β-catenin protein in both cytoplasmic and nuclear compartments. Interestingly, our results demonstrated that miR-1 overexpression led to a increase in cytoplasmic β-catenin levels and an increase reduction in its nuclear localization. Conversely, reintroduction of FAM83A resulted in a reversal of these effects (Fig. 3K–M). Overall,

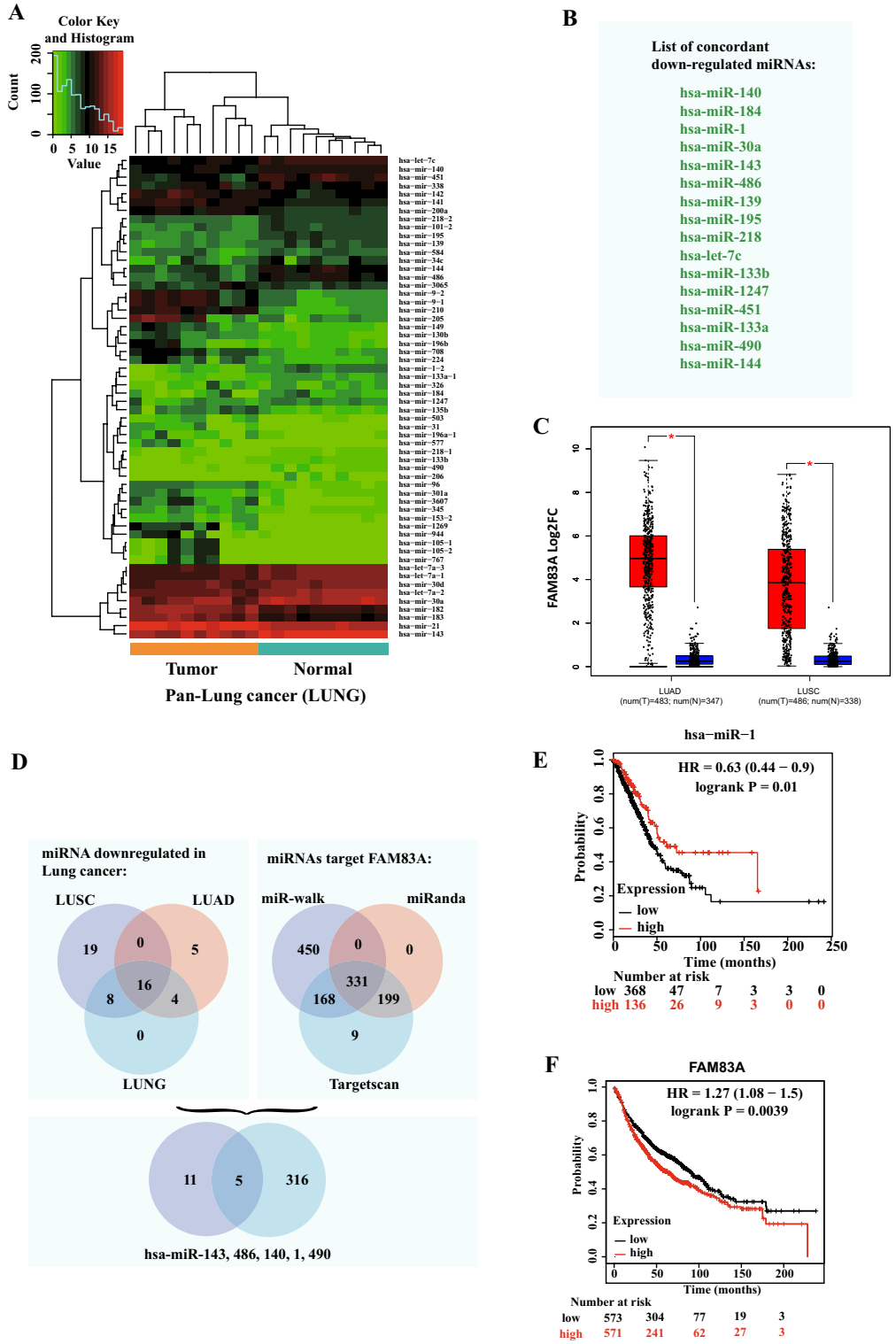

Figure 1. Identification of miR-1 as a negative regulator of FAM83A in human lung cancer. (**A**) Heatmap of the expression levels of miRNA in Pan-lung cancer. (**B**) List of concordant down-regulated miRNAs in lung cancer. (**C**) Relative expression levels of FAM83A in Lung adenocarcinoma (LUAD) and Lung squamous cell carcinoma (LUSC). (**D**) Venn diagram illustrating the overlap between downregulated miRNAs in lung cancer and FAM83A-targeted miRNAs. (**E**, **F**) Kaplan–Meier survival curves for miR-1 and FAM83A in lung cancer ($p < 0.05$).

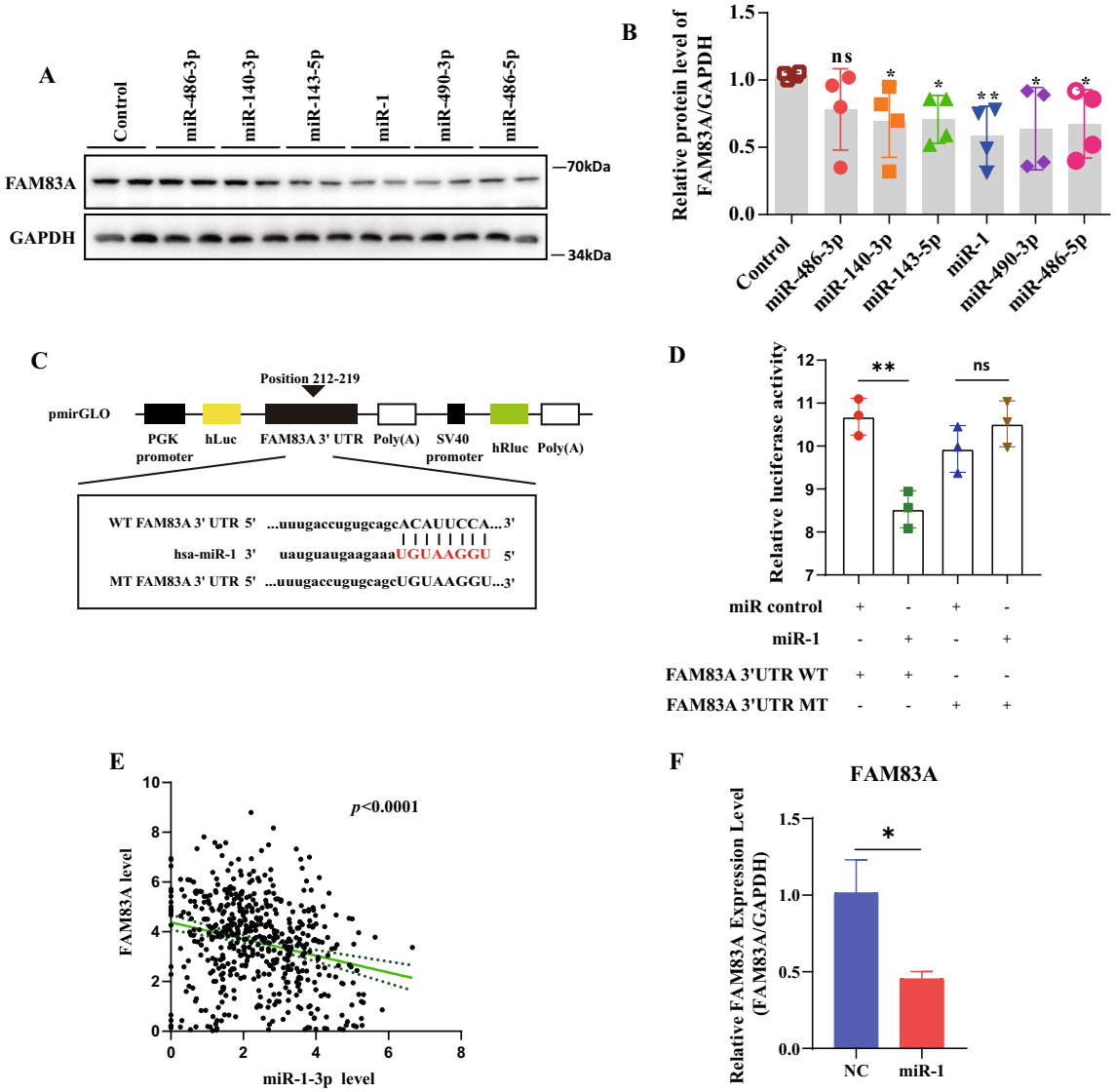

Figure 2. miR-1 directly targets FAM83A. (**A**) The expression of FAM83A by western blotting analysis after predicted miRNAs transfected in A549 for 48 h. GAPDH was used as a control. Blots were made from the same gel. (**B**) Quantification of FAM83A/GAPDH fold changes in Control and screened miRNAs. (**C**) Schematic illustration of predicted miR-1 binding sites within the 3'-UTR of FAM83A mRNA (position 212–219). (**D**) Luciferase activity was measured in lysates of HEK293T cells transfected with the wild-type 3′-UTR and mutant 3′-UTR of FAM83A luciferase constructs and a miR-1 mimic or a scrambled miRNA control. The luciferase activity was normalized to renilla luciferase activity. (**E**) miR-1 levels were inversely correlated with the levels of FAM83A in TCGA lung cancer database. (**F**) Relative mRNA levels of FAM83A after transfected with miR control and miR-1 mimics in A549 cells. All data are representative of 3 independent experiments. Data are represented as mean ± SD (n = 3). $^{*}p < 0.05$, $^{**}p < 0.01$, $^{***}p < 0.001$.

the findings of this part highlight the significance of miR-1 in reducing the nuclear translocation of β-catenin when inhibiting the Wnt/β-catenin signaling pathway through FAM83A.

miR-1 promotes the assembly of β-catenin degradation complex though FAM83A

The degradation complex of β-catenin plays a crucial role in regulating the stability of β-catenin, which is essential for activating the Wnt/β-catenin signaling pathway. In order to investigate how miR-1 affects the stability of the destruction complex through the FAM83A pathway, our study focused on examining whether miR-1 influences this process. Our results showed that overexpression of miR-1 led to a decrease in β-catenin protein levels, but when FAM83A was reintroduced, it restored the protein levels of β-catenin (Fig. 4A). Furthermore, overexpression of miR-1 accelerated the β-catenin degradation (Fig. 4B). The co-immunoprecipitation (co-IP) technique was employed to evaluate the interaction between GSK3β and β-catenin, which reflects the activity of the degradation complex responsible for β-catenin. The findings revealed that miR-1 overexpression augmented the binding capacity between GSK3β and β-catenin, thereby facilitating the formation of the degradation complex.

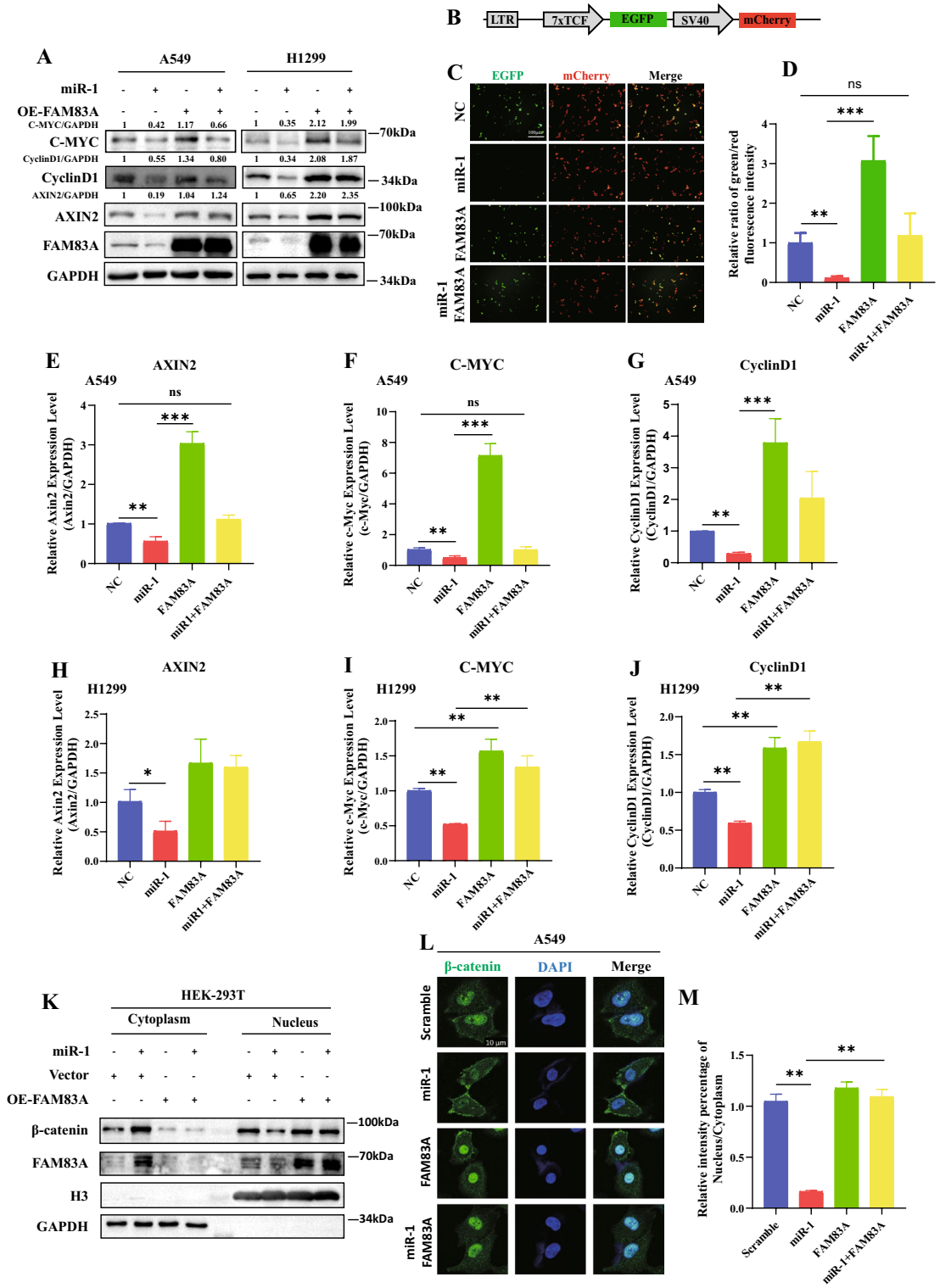

Figure 3. miR-1 decreases Wnt/β-catenin signal through FAM83A. (**A**) Western blotting analysis of Wnt/β-catenin signal target genes C-MYC, CyclinD1 and AXIN2 in A549 and H1299 cell lysates with or without miR-1 overexpression and re-expression FAM83A or vector. Representative western blotting images of 3 independent experiments. GAPDH was used as a control. Blots were made from the same gel. (**B**–**D**) The schematic diagram of 7TGC plasmid construction and the fluorescence images of HEK-293 T cells with or without miR-1 overexpression and re-expression FAM83A or vector. The relative ratio of green/red fluorescence intensity was quantified. (**E**–**J**) The mRNA level of Wnt/β-catenin signal target genes C-MYC, CyclinD1 and AXIN2 in A549 and H1299 cells with or without miR-1 overexpression and re-expression FAM83A or vector. (**K**) The protein level of cytoplasmic and nucleus β-catenin in HEK-293 T cells with or without miR-1 overexpression and re-expression FAM83A or vector were analyzed by western blotting. GAPDH was used as a cytoplasmic control. Histone H3 (H3) was used as a nucleus control. Representative western blotting images of 3 independent experiments. Blots were made from the same gel. (**L**, **M**) Distribution of β-catenin in A549 cells with or without miR-1 overexpression and re-expression FAM83A or vector. The relative ratio of nucleus/cytoplasm fluorescence intensity was quantified. Data are representative of 3 independent experiments. Data are represented as mean ± SD (n = 3). $^{*}p < 0.05$, $^{**}p < 0.01$,$^{***}p < 0.001$.

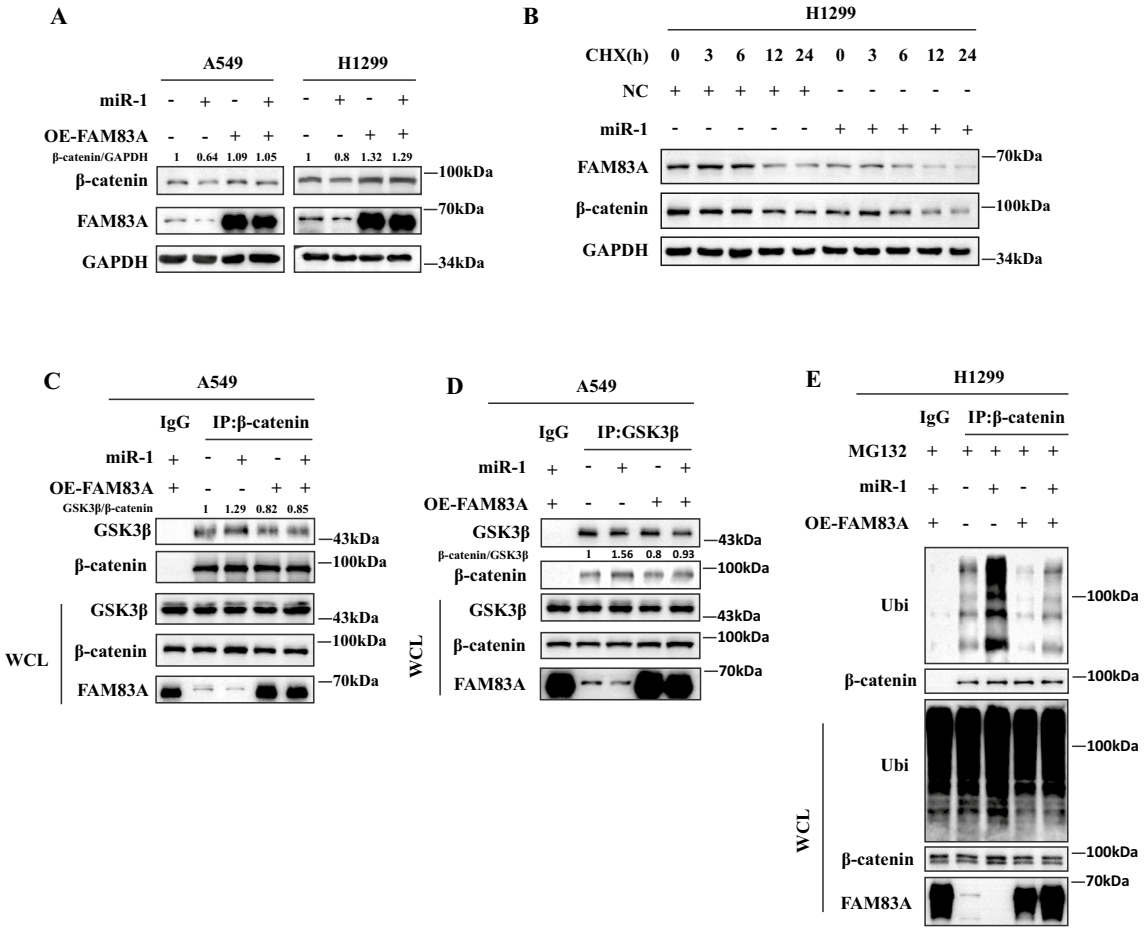

Figure 4. miR-1 inhibits the assembly of β-catenin degradation complex though FAM83A. (**A**) The protein level of β-catenin in A549 and H1299 cell lysates with or without miR-1 overexpression and re-expression FAM83A or vector were analyzed by western blotting. Representative western blotting images of 3 independent experiments. (**B**) Overexpression of miR-1 promoted the degradation of β-catenin protein upon cycloheximide (CHX, 20 μM) treatment for indicated times in H1299 cell lysates. Representative western blotting images of 3 independent experiments. (**C**, **D**) Representative immunoblots of endogenous GSK-3β and β-catenin in anti- β-catenin or anti- GSK-3β immunoprecipitates and lysates of A549 cells. Representative western blotting images of 3 independent experiments. (**E**) Ubiquitination of β-catenin was measured by Immunoprecipitation assay. H1299 cells were transfected with or without miR-1 overexpression and re-expression FAM83A or vector. Protein extracts were subjected to western blotting with indicated antibodies. Cells were treated with 10 μM MG132 for 6 h before being harvested. Representative western blotting images of 3 independent experiments. Blots in each subgroup were made from either the same gel or different gels with similar exposure times.

This effect could be counteracted by reintroducing FAM83A (Fig. 4C,D). The cells were subjected to MG132 treatment, which is a substance that inhibits proteasomes, in order to evaluate the degree of β-catenin ubiquitination after miR-1 was overexpressed. It was observed that the overexpression of miR-1 led to an increase in β-catenin ubiquitination levels, while the reintroduction of FAM83A reduced β-catenin ubiquitination and stabilized the protein level of β-catenin (Fig. 4E). The data presented above indicates that miR-1 has the potential to promote the formation of the β-catenin degradation complex through its interaction with FAM83A, leading to an expedited breakdown of β-catenin and ultimately resulting in the inhibition of the Wnt/β-catenin signaling pathway.

miR-1 inhibits human lung cancer proliferation, migration and invasion through FAM83A

To delve deeper into the involvement of miR-1 in NSCLC, we established a stable expression system for miR-1 in A549 and H1299 cell lines (Fig. S3A,B). Reversal of the observed phenomenon was achieved through the re-expression of FAM83A, which resulted in a slower migration rate for the miR-1 overexpression group compared to the negative control group in the wound healing experiment (Fig. 5A–D). MTT also exhibited a decline in the measured optical density (OD) value, indicating a reduction in cellular proliferation capacity (Fig. 5E,F). The Edu incorporation assay revealed a notable decrease in DNA synthesis capacity in H1299 and A549 cells upon miR-1 overexpression, as opposed to the control group. Intriguingly, reintroducing FAM83A reinstated the proliferative potential of both H1299 and A549 cells (Fig. 5G–J). The results of the colony formation assay indicated that the inhibitory effect of miR-1 on clone numbers could be counteracted by restoring FAM83A expression

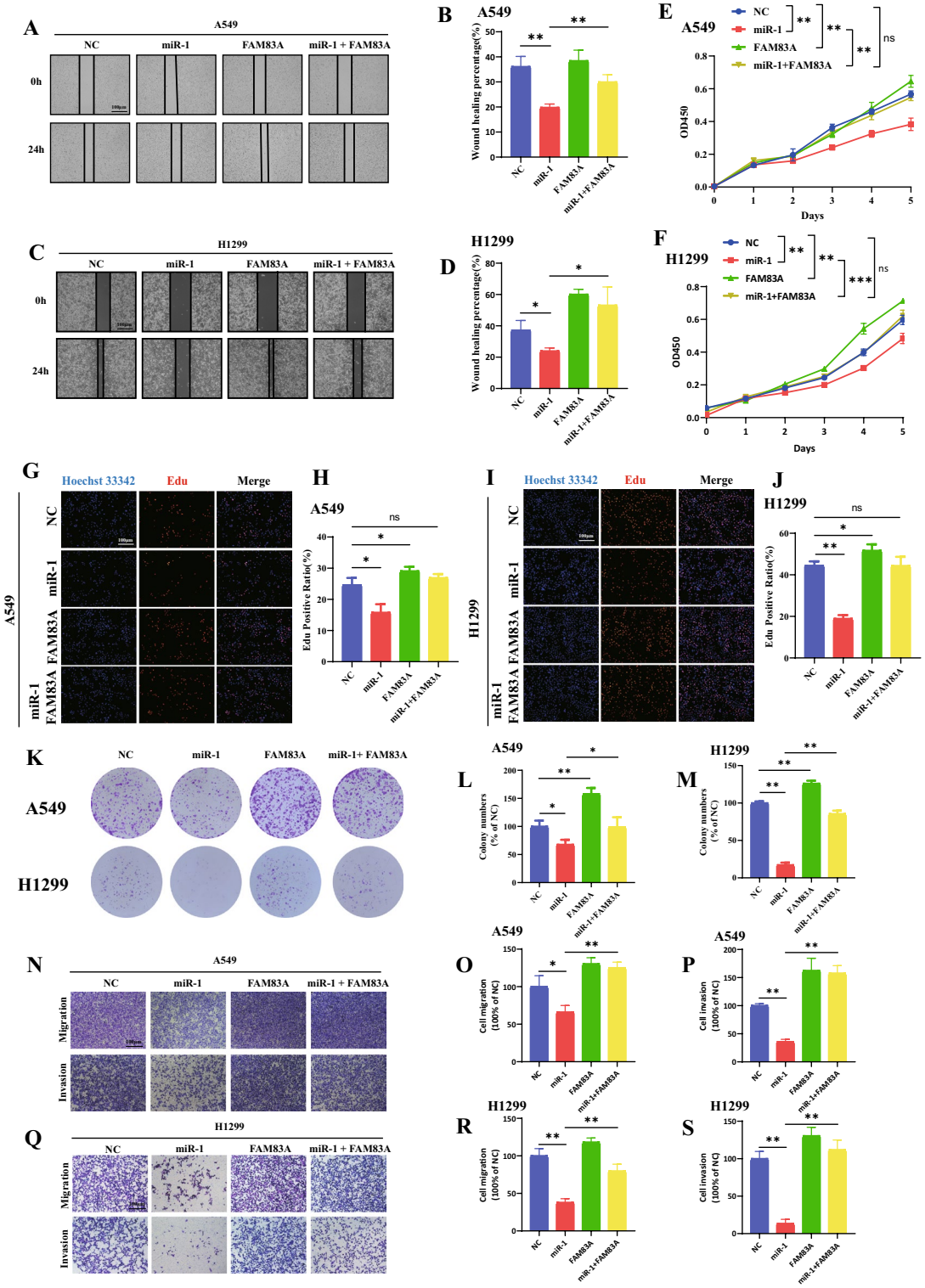

Figure 5. miR-1 inhibits human lung cancer cell proliferation, migration and invasion through FAM83A. (**A**–**D**) Wound scratch assay for A549 and H1299 cells were transfected with or without miR-1 overexpression and re-expression FAM83A or vector with indicated time points and the quantification was done for % migration ratio. (**E**, **F**) MTT assay for A549 and H1299 cells were transfected with or without miR-1 overexpression and re-expression FAM83A or vector. (**G**–**J**) EdU staining assay for evaluation of the influences of A549 and H1299 cells were transfected with or without miR-1 overexpression and re-expression FAM83A or vector. (**K**–**M**) Colony formation was used for the measurement of A549 and H1299 cells were transfected with or without miR-1 overexpression and re-expression FAM83A or vector and the quantification was done for the number of colonies. (**N**–**S**) Transwell assay was used to detect A549 and H1299 cells were transfected with or without miR-1 overexpression and re-expression FAM83A or vector migration and invasion. Representative images of migration and invasion of each cell group are shown. All data are representative of 3 independent experiments. Data are represented as mean ± SD (n = 3). $^{*}p < 0.05$,$^{**}p < 0.01$,$^{***}p < 0.001$.

(Fig. 5K–M). Meanwhile, the overexpression of miR-1 was found to suppress the migratory and invasive abilities of H1299 and A549 cells, as demonstrated by transwell assays (Fig. 5N–S). These findings collectively indicate that FAM83A is targeted by miR-1 to inhibit proliferation, migration, and invasion in H1299 and A549 cells.

Discussion

The NSCLC exhibits a substantial increase in the activation of the canonical Wnt signaling pathway, which plays a crucial role in facilitating cellular proliferation, migration, and invasion[1]. The upregulation of FAM83A expression is notably observed in lung cancer. However, despite limited understanding, substantial evidence exists to support the involvement of FAM83A in the promotion of lung cancer by activating the Wnt/β-catenin signaling pathway and subsequently augmenting cellular proliferation[13]. In our previous study, we presented evidence of the interplay between FAM83A and β-catenin facilitated by the DUF1669 domain, underscoring its pivotal function in impeding the formation of the β-catenin degradation complex, Facilitating the nuclear translocation of β-catenin and upholding β-catenin stability[4]. Additionally, FAM83A has been shown to design inhibitory peptides with significant implications for cancer therapy[4]. The results suggest that FAM83A represents a promising target for effective cancer therapy.

Effective targeting of FAM83A has been observed with miR-1, which exhibits significant down-regulation in patients diagnosed with lung cancer. In H1299 and A549 cells line, we confirmed that miR-1 attenuated the expression of Wnt downstream target genes by suppressing FAM83A. GSK3β phosphorylates β-catenin at the amino terminus serine/threonine residues, leading to its binding with β-Trcp protein that undergoes covalent ubiquitination and subsequent proteasomal degradation[1]. Therefore, the interaction between GSK3β and β-catenin plays a vital role in the degradation process of β-catenin through ubiquitination. In this study, we present evidence that miR-1 suppresses FAM83A expression to enhance the functionality of the β-catenin degradation complex, leading to reduced proliferation, migration, and invasion capabilities in NSCLC cells. Consequently, this promotes the translocation of β-catenin into the nucleus (Fig. 6).

The RNA-based therapeutic approach precisely targets and modulates the activity of endogenous miRNAs to regulate gene expression. Given the pivotal role of miRNAs in both normal physiological processes and pathological conditions, miRNA therapy aims to restore miRNA expression homeostasis by specifically targeting and manipulating specific miRNAs[14]. RNA-based therapy represents a promising therapeutic modality for currently incurable diseases, particularly in the realm of cancer treatment[5]. With the advancement of miRNA nano-delivery technology, RNA-based molecular therapy has been implemented in clinical cancer treatment[15]. Hence, it is crucial to thoroughly examine miRNAs with outstanding precision and maximum effectiveness as potential therapeutic agents for diverse ailments. In this investigation, we performed an extensive assessment of miR-1 interaction with FAM83A by employing both database analysis and experimental verification. The dysregulation of miR-1 in lung cancer is intricately associated with the initiation and progression of this malignancy. Notably, the downregulation of miR-1 emerges as a pivotal factor facilitating the advancement of lung cancer. Previous

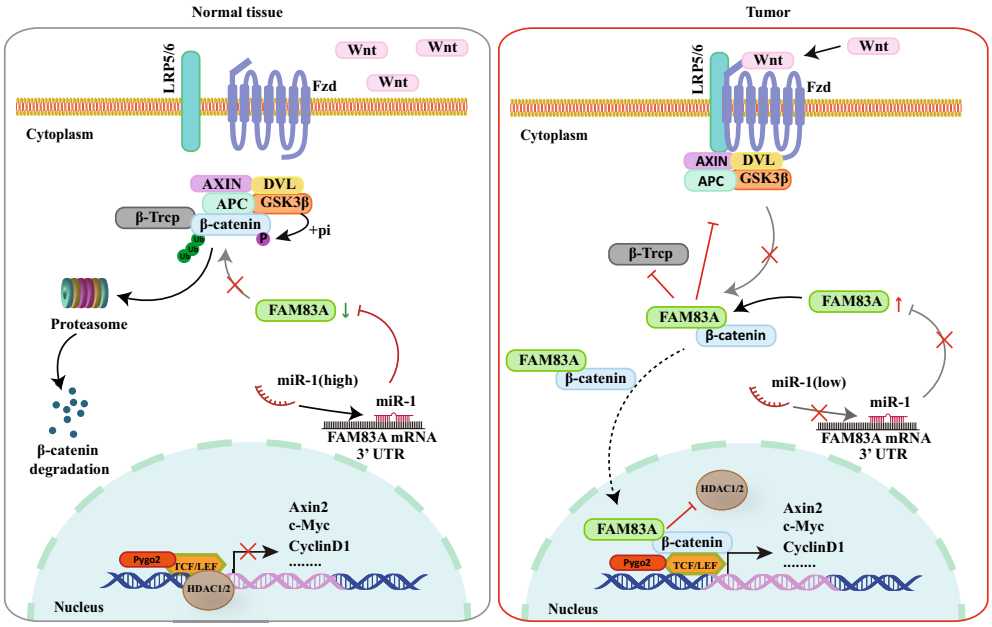

Figure 6. The proposed mechanism by which miR-1 inhibits NSCLC involves the FAM83A/Wnt/β-catenin pathway. In the cytoplasm, miR-1 targets FAM83A mRNA, leading to a decrease in FAM83A protein levels. Consequently, β-catenin fails to be stabilized by FAM83A and undergoes degradation through the ubiquitin–proteasome pathway. Furthermore, miR-1-mediated reduction of FAM83A levels results in diminished nuclear import of β-catenin, thereby attenuating the transcriptional targets associated with downstream WNT signaling. In conclusion, miR-1 suppresses NSCLC progression by targeting FAM83A and inhibiting the WNT pathway.

studies have demonstrated that downregulation of miR-1 promotes the upregulation of AXIN2, CyclinD1, and other related proteins in lung cancer cells, thereby facilitating the proliferation of these cells[16]. This discovery suggests a possible link between the decrease in miR-1 and the initiation of the Wnt/β-catenin signaling pathway. Therefore, manipulating the expression level of miR-1 could offer a potential targeted therapeutic strategy for addressing lung cancer[17]. While the inhibitory effects of the miRNA-1-FAM83A axis on lung cancer growth and metastasis have been established in previous studies, there is still a need to further elucidate its underlying mechanism comprehensively[18]. Here, we have further investigated the regulatory mechanism of the miRNA-1-FAM83A axis in promoting lung cancer cell growth and demonstrated the potential anti-lung cancer properties of miRNA-1 through its ability to target FAM83A. Our findings suggest that miRNA-1 enhances the activity of a complex responsible for degrading β-catenin, leading to inhibition of the Wnt/β-catenin signaling pathway.

In the past few years, there has been a significant amount of research conducted on miR-1 and its impact on different physiological processes and diseases. These studies have shown that miR-1 is often down-regulated in various types of cancer, suggesting its potential role in the development of tumors[19]. Animal studies have demonstrated a significant down-regulation of miR-1 in the mouse model of ethyl carbamate induced lung cancer[20]. Recently, there has been an observation of decreased levels of miR-1 in tumor tissues and serum samples obtained from patients diagnosed with small cell lung cancer. This finding highlights the importance of miR-1 as a significant biomarker for the progression and spread of tumors. The introduction of miR-1 into cell lines associated with small cell lung cancer led to a notable decrease in both the growth and metastasis of tumor cells. In terms of mechanism, it was discovered that miR-1 directly targets CXCR4, thereby impeding ability of FOXM1 to bind to the RRM2 promoter. Consequently, this inhibition effectively suppresses the growth and metastasis of lung cancer cells[21]. The regulatory role of miR-1 in tumor cells encompasses multiple facets, including targeting resistance mechanisms, apoptosis pathways, and immune-related genes to effectively impede tumor cell proliferation[22–24]. The progression of tumors arises from intricate and multifaceted interactions between malignant cells and their microenvironment[25]. Exosomes are extracellular vesicles consisting of phospholipid bilayers that are ubiquitous in various body fluids, carrying miRNA information from parental cells and communicating with recipient cells through binding to their corresponding ligands[26]. Exosomal miRNAs have been demonstrated to exert an influence on the tumor microenvironment through modulation of the extracellular matrix and immune system, thus extensively investigated as potential tumor biomarkers[27,28]. For instance, the presence of exosomal has-miR-1-3p in cerebrospinal fluid can serve as a valuable biomarker for assessing non-small cell lung cancer metastasis, and the expression level of miR-1 gradually escalates over the course of treatment[29]. This observation may be attributed to the ability of miR-1 to modulate the epithelial-mesenchymal transition (EMT) process in cancer cell[30]. Cumulatively, these lines of evidence indicate that miR-1 plays a pivotal role in facilitating tumor cell proliferation, migration, and invasion.

Reversing the abnormal activation of the Wnt/β-catenin signaling pathway is crucial in combating a wide range of human cancers, making it an essential focus for pharmacological intervention. FAM83A plays a vital role in modulating the Wnt/β-catenin signaling pathway. In brief, our results shed light on how miR-1 hinders the advancement of lung cancer by directly targeting the FAM83A/Wnt/β-catenin pathway. Importantly, our results provide a rationale for RNA-based therapeutic strategies aimed at targeting miR-1 to combat lung cancer development.

Experimental procedures

Cell lines, reagents, and antibodies

Human non-small cell lung cancer cell line A549, H1299 and HEK293T were purchased from the National Collection of Authenticated Cell Cultures, Chinese Academy of Science (SCSP-538, SCSP-589 and GNHu44) and stored in our lab. HEK293T, A549 and H1299 cells were cultured in Dulbecco's modified Eagle's medium (DMEM) (G4515, Servicebio, China). All culture mediums were supplemented with 10% fetal bovine serum (G10270-106, Gibco, USA), 100 U/ml penicillin G and 100 μg/ml streptomycin (P1400, Solarbio) at 37 °C in a humidified incubator containing 5% CO2. The medium was replaced every 2–3 days and the cell was subcultured and used for an experiment at 80–90% confluence. Commercially available antibodies and dilutions used are as follows:anti-FAM83A (Proteintech, 20,618-1-AP; 1:1000 dilution), anti-GAPDH (Proteintech, 60,004-1-Ig; 1:5000 dilution),anti-C-MYC (Proteintech, 10,828-1-AP; 1:1000 dilution),anti-CyclinD1 (Proteintech, 60,186-1-Ig; 1:5000 dilution),anti-AXIN2 (Proteintech, 20,540–1-AP; 1:1000 dilution),anti-β-catenin(Proteintech, 51,067-2-AP; 1:1000 dilution),anti-Histone H3(Proteintech, 17,168–1-AP; 1:1000 dilution),Anti-GSK3β (Cell Signaling Technology, 9315S; 1:1000 dilution),Anti-Ubi (MBL, MK-12-3; 1:1000 dilution). 7TGC was kind given from RoelNusse (Addgene, 24304). miRNA-143-5p minics, miRNA-486-3p minics, miRNA-486-5p minics, miRNA-140-3p minics, miRNA-1 minics, miRNA-490-3p and miR control were designed and synthesized by GenePharma (Shanghai, China).

Lentiviral production and creation of stable cell lines

Pre-miR-1 or scramble RNA were subcloned into the lentiviral vector pCDH-CMV-MCS-EF1-turboRFP-T2A-puro. DNA fragments encoding FAM83A were subcloned into lentiviruses vector pLVX-IRES-Neo. 5 μg lentiviral constructs were co-transfected with viral packaging plasmids 3 μg psPAX2 and 3 μg pMD2.G into 293 T cells in 10 cm dishes for the lentiviral particle production. The viral supernatant was harvested at 48 h and 72 h post-transfection and filtered through a 0.22 μm membrane. After applying the viral supernatant to A549 and H1299 cells with 10 μg/μl of polybrene (Solarbio, H8761), selection for puromycin and/or G418 resistance was initiated 48 h after transfection. The selection media was changed every 3–4 days for several weeks, and clones of puromycin and/or G418—resistant cells were isolated and expanded for further characterization. The stable

cells were maintained with complete culture medium with 2 μg/mL puromycin (Beyotime, ST551) and/or 100 μg/mL G418 (Yeasen, 60220ES03).

Dual-luciferase reporter assay
To assess the regulatory effects of miR-1 on FAM83A mRNA, dual-luciferase reporter assay was performed. the 3′UTR of FAM83A containing 212–219 bp and mutant were synthesized by Sangon Biotech and cloned between the SacI and XbaI sites of the pmiRGLO dual-luciferase miRNA target expression vector (Promega, E1330). The primer sequences specific to FAM83A 3′UTR used for the dual-luciferase reporter assay were (forward) 5′-CTTTGACCTGTGCAGCACATTCCAGAAGGTTCCAGGGAGGTTGT-3′ and (reverse) 5′-CTAGACAACCTCCCTGGAACCTTCTGGAATGTGCTGCACAGGTCAAAGAGCT-3′. The FAM83A 3′UTR mutant primer sequences were (forward) 5′-CTTTGACCTGTGCAGCTGTAAGGTGAAGGTTCCAGGGAGGTTGT-3′ and (reverse) 5′-CTAGACAACCTCCCTGGAACCTTCACCTTACAGCTGCACAGGTCAAAGAGCT-3′.

RNA extraction and real-time PCR
Total RNA was isolated from cells using TRIzol reagent (Invirogen) according to the manufacturer's protocol. RNAs were quantified using a NanoDrop One instrument (ThermoFisher). cDNA was reverse transcribed using a miRNA 1st Strand cDNA Synthesis Kit (by stem-loop) (Vazyme, MR101-01). Primers for miR-1 reverse transcription: GTCGTATCCAGTGCAGGGTCCGAGGTATTCGCACTGGATACGACATACAT. For gene expression analysis, real-time PCR was performed using a QuantStudio 3 instrument (Thermo, USA) and miRNA Universal SYBR qPCR Master Mix (Vazyme, MQ101-02). Expression of microRNAs was normalized to that U6 shRNA. The sequences of the primers used in real-time PCR were shown in Table 1.

Wound-healing assay
A549 and H1299 cells transfected with or without miR-1 overexpression and re-expression FAM83A or vector were cultured after the formation until 80% confluence, then the surface of monolayers was scratched with pipette tips. PBS was used to move cell debris and the conditioned medium was added. After healing for 24 h, the scratches at the same wound location were observed and pictured under an Olympus FSX100 microscope.

Transwell assay
For migration, A549 and H1299 cells transfected with or without miR-1 overexpression and re-expression FAM83A or vector were seeded in upper transwell chamber (Corning Incorporated, #3422) with 1×10^5 cells in 100uL of FBS-free medium. For invasion, transwell chamber pre-covered with Matrigel (Corning Incorporated, 356234) was used. Meanwhile, 500μL of medium containing 20% FBS was added to the lower cavity. 24 h later, the cells were fixed by 0.1% crystal violet and stained by 4% PFA Fix Solution. Under microscope, the number of invasive cells from 3 fields was counted.

MTT assay
A549 and H1299 cells (1×10^3 cells/well) transfected with or without miR-1 overexpression and re-expression FAM83A or vector were seeded into 96-well plates, then cells were stained at the indicated time points with 100 μL sterile MTT dye (0.5 mg/ml; Sigma, M2128) for 4 h at 37 °C. After adding 150 μL DMSO (Biosharp, BS186), the number of viable cells was assessed by measurement of the absorbance at 450 nm by a microplate reader. All experiments were performed in triplicate.

Colony formation assay
A549 and H1299 cells transfected with or without miR-1 overexpression and re-expression FAM83A or vector were seeded into a 12-well plate and incubated with complete medium at 37 °C for 2–3 weeks. Then, the cells were fixed with 4% paraformaldehyde and stained with 2% crystal violet. Images were obtained and the number of colonies was counted.

Immunoprecipitation assay
Cells were washed twice with phosphate-buffered saline (PBS; Servicebio, WGSH30256-01) and lysed with RIPA lysis buffer (50 mM Tris–HCl pH 7.4, 150 mM NaCl, 1% Triton X-100 [Sangon Biotech, 9002-93-1], 10 mM NaF, and 1 mM EDTA) containing proteinase inhibitor cocktail (Biomake, B14001). Protein concentration was

Gene	Forward 5′-3′	Reverse 5′-3′
miR-1	GCGCGTGGAATGTAAAGAAGT	AGTGCAGGGTCCGAGGTATT
U6	CTCGCTTCGGCAGCACA	AACGCTTCACGAATTTGCGT
FAM83A	ATCCGGAGTGTGGAAGGAGAG	TCCAGACAGGACAAATCTCCAGT
C-MYC	GCCACGTCTCCACACATCAG	TGGTGCATTTTCGGTTGTTG
CyclinD1	TCAAGTGTGACCCGGACTGCCT	GCACGTCGGTGGGTGTGCAA
AXIN2	ATTCGGCCACTGTTCAGACG	GACAACCAACTCACTGGCCTG

Table 1. The RT-qPCR primer sequences used in this study.

measured using a BioRad Protein Assay kit (BioRad, 5,000,006). Cell lysates were incubated overnight with primary antibodies according to each individual experiment after pretreatment with IgG and protein A/G magic beads (Bimake, B23202), and then incubated with protein A/G magic beads for 2 h at 4 °C. The beads were spun down and washed five or six times, and the Enhanced BCA Protein Assay Kit (Beyotime, P0009) was used to detect the concentration of proteins. For the ubiquitination assay, before collection with the denaturation buffer (10 mM imidazole, 0.1 M Na_2HPO_4/NaH_2PO_4 and 6 M guanidine- HCl), cells were treated with 10 μM MG132 for 6 h. The lysates were mixed with the indicated antibodies at 4 °C overnight, followed by washes and western blotting assay.

Immunofluorescence and confocal microscopy
A549 cells transfected with the appropriate plasmids were grown on 12-well plates, and for confocal microscopy on glass chambers, at 60% density and cultured for 48 h. Cells were fixed with 4% paraformaldehyde in PBS and permeabilized with 0.5% Triton X-100. Then cells were blocked with 10% goat serum (Boster, AR0009) and subsequently incubated with primary antibodies and fluorescence-labeled secondary antibodies. DAPI (Solarbio, C0065) was used for nuclei staining. For confocal microscopy, cells plated on the glass chambers were examined with a confocal laser-scanning microscope (Leica SP8, Wetzlar, Germany) using a 63 × oil immersion objective. Data analysis was performed using the Leica LAS AF Lite software.

5-ethynyl-20-deoxyuridine (EdU) incorporation assay
EdU labeled A549 and H1299 transfected with or without miR-1 overexpression and re-expression FAM83A or vector were examined with the BeyoClick™ EdU Cell Proliferation Kit with Alexa Fluor 555 (Beyotime, C0075S). Cells were photographed under an Olympus FSX100 microscope.

Western blot analysis
Cell lysates or immunoprecipitates were heated in 1 × SDS loading buffer (100 mM Tris–HCl [pH 6.8], 4% [wt:vol] SDS, 200 mM dithiothreitol, 0.2% [wt:vol] bromophenol blue, and 20% [vol:vol] glycerol) for 15 min at 98 °C. Proteins were separated by SDS-PAGE gels and transferred to 0.45 μm polyvinylidene fluoride (PVDF) membranes (Millipore, IPFL85R). After the PVDF membranes had been blocked with TBS-T containing 5% skimmed milk at room temperature for 2 h and incubated with primary antibodies and secondary antibodies, the protein signals in the PVDF membranes were detected using SuperPico ECL Chemiluminescence Kit (Vazyme, E422-02) according to the manufacturer's instructions.

Statistical analysis
All experiments were performed independently at least three times. All statistical analysis was performed using GraphPad Prism 8.0 software (GraphPad, La Jolla, CA, USA). All data are presented as mean ± SD (standard deviation) from triplicates. p values < 0.05 were statistically significant. Statistical analysis was done using paired Student's t-test; *represents $P < 0.05$, **represents $P < 0.01$ and ***represents $P < 0.001$.

Data availability
The data that support the findings of this study are available from the corresponding author upon reasonable request.

Received: 24 April 2024; Accepted: 15 July 2024
Published online: 29 July 2024

References
1. Stewart, D. J. Wnt signaling pathway in non-small cell lung cancer. *J. Natl. Cancer. Inst.* **106**, djt356 (2014).
2. Nusse, R. & Clevers, H. Wnt/beta-catenin signaling, disease, and emerging therapeutic modalities. *Cell.* **169**, 985–999 (2017).
3. Li, Y. *et al.* BJ-TSA-9, a novel human tumor-specific gene, has potential as a biomarker of lung cancer. *Neoplasia.* **7**, 1073–1080 (2005).
4. Zhou, C. *et al.* B-lymphoid tyrosine kinase-mediated FAM83a phosphorylation elevates pancreatic tumorigenesis through interacting with beta-catenin. *Signal Transduct. Target. Ther.* **8**, 66 (2023).
5. Kim, D. H. & Rossi, J. J. Strategies for silencing human disease using RNA interference. *Nat. Rev. Genet.* **8**, 173–184 (2007).
6. Sahin, U., Kariko, K. & Tureci, O. MRNA-based therapeutics-developing a new class of drugs. *Nat. Rev. Drug Discov.* **13**, 759–780 (2014).
7. Ambros, V. The functions of animal MicroRNAs. *Nature.* **431**, 350–355 (2004).
8. Shukla, G. C., Singh, J. & Barik, S. MicroRNAs: Processing, maturation, target recognition and regulatory functions. *Mol. Cell Pharmacol.* **3**, 83–92 (2011).
9. Lee, Y. S. & Dutta, A. MicroRNAs in cancer. *Annu. Rev. Pathol.* **4**, 199–227 (2009).
10. Lee, R. C., Feinbaum, R. L. & Ambros, V. The *C. elegans* heterochronic gene lin-4 encodes small RNAs with antisense complementarity to lin-14. *Cell.* **75**, 843–854 (1993).
11. Hill, M. & Tran, N. MiRNA interplay: Mechanisms and consequences in cancer. *Dis. Model. Mech.* **14**, dmm047662 (2021).
12. Khan, P. *et al.* MicroRNA-1: Diverse role of a small player in multiple cancers. *Semin. Cell Dev. Biol.* **124**, 114–126 (2022).
13. Zheng, Y. W. *et al.* FAM83a promotes lung cancer progression by regulating the Wnt and Hippo signaling pathways and indicates poor prognosis. *Front. Oncol.* **10**, 180 (2020).
14. Seyhan, A. A. Trials and tribulations of MicroRNA therapeutics. *Int. J. Mol. Sci.* **25**, 1469 (2024).
15. Ganju, A. *et al.* MiRNA nanotherapeutics for cancer. *Drug Discov. Today.* **22**, 424–432 (2017).
16. Dai, S., Li, F., Xu, S., Hu, J. & Gao, L. The important role of MiR-1-3P in cancers. *J. Transl. Med.* **21**, 769 (2023).
17. Wang, Y., Luo, X., Liu, Y., Han, G. & Sun, D. Long noncoding RNA RMRP promotes proliferation and invasion via targeting MiR-1-3P in non-small-cell lung cancer. *J. Cell. Biochem.* **120**, 15170–15181 (2019).

18. Liu, P. J. *et al.* Involvement of MicroRNA-1-FAM83a axis dysfunction in the growth and motility of lung cancer cells. *Int. J. Mol. Sci.* **21**, 8833 (2020).
19. Safa, A. *et al.* MiR-1: A comprehensive review of its role in normal development and diverse disorders. *Biomed. Pharmacother.* **132**, 110903 (2020).
20. Melkamu, T., Zhang, X., Tan, J., Zeng, Y. & Kassie, F. Alteration of MicroRNA expression in vinyl carbamate-induced mouse lung tumors and modulation by the chemopreventive agent indole-3-carbinol. *Carcinogenesis.* **31**, 252–258 (2010).
21. Khan, P. *et al.* MicroRNA-1 attenuates the growth and metastasis of small cell lung cancer through CXCR4/FOXM1/RRM2 axis. *Mol. Cancer.* **22**, 1 (2023).
22. Wu, Y., Pu, N., Su, W., Yang, X. & Xing, C. Downregulation of MiR-1 in colorectal cancer promotes radioresistance and aggressive phenotypes. *J. Cancer.* **11**, 4832–4840 (2020).
23. Peng, J. *et al.* Upregulation of MicroRNA-1 inhibits proliferation and metastasis of breast cancer. *Mol. Med. Rep.* **22**, 454–464 (2020).
24. Li, D. *et al.* Programmed death ligand-1 (PD-L1) regulated by NRF-2/MicroRNA-1 regulatory axis enhances drug resistance and promotes tumorigenic properties in sorafenib-resistant hepatoma cells. *Oncol. Res.* **28**, 467–481 (2020).
25. Quail, D. F. & Joyce, J. A. Microenvironmental regulation of tumor progression and metastasis. *Nat. Med.* **19**, 1423–1437 (2013).
26. Li, B., Cao, Y., Sun, M. & Feng, H. Expression, regulation, and function of exosome-derived MiRNAs in cancer progression and therapy. *Faseb. J.* **35**, e21916 (2021).
27. Sun, Z. *et al.* Effect of exosomal MiRNA on cancer biology and clinical applications. *Mol. Cancer.* **17**, 147 (2018).
28. Li, J. *et al.* Exosome detection via surface-enhanced Raman spectroscopy for cancer diagnosis. *Acta Biomater.* **144**, 1–14 (2022).
29. Li, H. et al. Cerebrospinal fluid exosomal MicroRNAs as biomarkers for diagnosing or monitoring the progression of non-small cell lung cancer with leptomeningeal metastases. *Biotechnol. Genet. Eng. Rev.* 1–22 (2023).
30. Han, C. *et al.* MicroRNA-1 (MiR-1) inhibits gastric cancer cell proliferation and migration by targeting MET. *Tumour Biol.* **36**, 6715–6723 (2015).

Author contributions

W.Y., wrote the manuscript and performed molecular biology experiments. J.T. and C.Z. designed the whole project and supervised all experiments. W.Y., W.L., H.H., X.C., R.Z., H.L., S.X., D.G. and Q.Z. conducted all experiments and analyzed the data. D.W. and M.M., X.-Z.C., provided support with experimental and clinical techniques. All authors read and approved the final manuscript. All authors consent to publication.

Funding

This work was supported by the National Natural Science Foundation of China (82273970 and 32070726 to J.F.T., 32270768 to C.F.Z., 82370715 to X.Z.C.), Innovation Group Project of Hubei Province (2023AFA026 to J.F.T.), The National Key R&D Program of China (2023YFC2507900).

Competing interests

The authors declare no competing interests.

Additional information

Supplementary Information The online version contains supplementary material available at https://doi.org/10.1038/s41598-024-67686-3.

Correspondence and requests for materials should be addressed to C.Z. or J.T.

Reprints and permissions information is available at www.nature.com/reprints.

Publisher's note Springer Nature remains neutral with regard to jurisdictional claims in published maps and institutional affiliations.